Pharmaceutical Research, Vol. 27, No. 3, March 2010 (© 2010)
DOI: 10.1007/s11095-009-0032-y

Research Paper

Oxidation of Free L-histidine by *tert*-Butylhydroperoxide

Bruce D. Mason,[1] Melissa McCracken,[1] Edward J. Bures,[1] and Bruce A. Kerwin[2,3]

Received October 5, 2009; accepted December 7, 2009; published online February 2, 2010

Purpose. L-histidine, a commonly used buffer for protein formulations, has the potential to oxidize and form multiple byproducts. Previous studies were performed using metal catalyzed oxidation with Fe^{2+} or Cu^{2+}. We re-examined the oxidation of L-histidine under conditions more appropriate to protein formulations.
Methods. Solutions of free L-histidine, protected from light, were initially reacted with *tert*-butylhydroperoxide and the products analyzed by UV absorption spectroscopy, reversed phase HPLC and mass spectrometric analysis and NMR. Experimental parameters investigated were oxidizing agent, pH, temperature, metal ion and metal chelator content.
Results. The initial reaction produced a number of known products, along with an unknown product that was identified as 4(5)-imidazolecarboxaldehyde. The reaction was highly pH and oxidizing-agent specific. The product was not observed at pH 5.0 or below, while there was a dramatic increase for reactions carried out at pH 6.0 or above. Addition of $FeSO_4$ to the reaction dramatically increased the amount of 4(5)-imidazolecarboxaldehyde produced, while addition of the metal chelators EDTA or DTPA completely inhibited the reaction.
Conclusions. The presence of oxidants and trace concentrations of metal ions in high purity L-histidine solutions results in the formation of 4(5)-imidazolecarboxaldehyde which has the potential to covalently modify proteins.

KEY WORDS: histidine; metal catalyzed oxidation; metal chelators; tert-butylhydroperoxide; 4(5)-imidazolecarboxaldehyde.

INTRODUCTION

L-histidine has the potential to oxidize through a wide variety of mechanisms. The most common oxidation mechanism observed is photooxidation, which produces a yellowing of aqueous solutions upon extended exposure to ambient light. The byproduct(s) responsible for producing the yellow color have not been elucidated in any publications, although its presence has been noted in publications describing protein formulations (1). L-histidine is susceptible to singlet molecular oxygen-mediated photooxidation, which is also known as the "photodynamic effect" (2–5). The attack by singlet oxygen on L-histidine occurs at the imidazole ring via unstable endoperoxide intermediates (6,7), resulting in a large variety of products, most of which are unstable and occur as intermediates for the overall reaction. Of the over 25 known photodegradation products, aspartic acid and urea are the most common end products (8).

L-histidine is also commonly known to form chelates with ditrivalent and trivalent metal cations. In fact, Chen *et. al.* have cautioned against storage of L-histidine HCl solutions in stainless steel vessels as there is the potential for the chloride ions to corrode the stainless steel and cause iron to be leached into the solution (1). Because of this propensity to bind metals, many studies have examined the metal catalyzed oxidation products of L-histidine, such as the Fenton reaction upon addition of metal cations. The Fenton system consists of Fe^{2+} and hydrogen peroxide in the presence of bicarbonate ion generating hydroxyl radicals that can attack the amino acid and lead to modifications (9–12). In general, the products from the oxidation of amino acids by Fenton chemistry are NH_4^+, carbon dioxide, oximes, α-ketoacids and upon the loss of a carbonyl, the corresponding aldehyde, which is further oxidized to a carboxylic acid (13,14). Known metal catalyzed oxidation products of L-histidine include aspartate, 2-oxohistidine, (15,16) imidazole pyruvic acid, (17,18), 4(5)-imidazole acetaldehyde (19–22), 4(5)-imidazole acetic acid (23), imidazole lactic acid (23), 4(5)-imidazole acetonitrile (19,20,24,25), and β-imidazolylpyruvic acid (17,18).

While L-histidine-containing solutions can be protected from light and chelators added to prevent hydroxyl radical formation and eliminate potential metal-catalyzed oxidation, peroxide formation still occurs. Polysorbates typically contain peroxides, which are commonly used during purification of membrane proteins (26,27) and in solutions for storage of purified proteins (28). The pH of many protein storage solutions is in the range of 5–7 (29), making L-histidine an

[1] Amgen Inc., Process and Product Development, Analytical and Formulation Sciences Group, Thousand Oaks, California 91320, USA.
[2] Amgen Inc., Process and Product Development, Analytical and Formulation Sciences Group, Seattle, Washington 98101, USA.
[3] To whom correspondence should be addressed. (e-mail: bkerwin@amgen.com)

attractive buffer, as it has a pKa of 6.0 on its imidazole group. Because of its pH buffering properties, its low volatility and minimal pH change upon freezing, it has been used extensively in lyophilized protein formulations (30). L-histidine has historically been used only sparingly in liquid formulations of proteins, although lately it has gained more prominence for its use including those for monoclonal antibodies (1) and cytokines (31,32). To our knowledge, there is a scarcity of available information on the reaction between inorganic and organic peroxides with free L-histidine. Therefore, in the current study, the oxidation of L-histidine was re-examined under conditions more appropriate to protein storage solutions using high purity L-histidine without intentionally adding metal cations. Past work has been done examining this system using chemiluminescence, but the reaction products were reported simply as carbonyls and were not fully characterized beyond this point (33). Here, we report that free L-histidine is degraded by *tert*-butylhydroperoxide in a pH- and temperature-dependent manner to form 4(5)-imidazolecarboxaldehyde, imidazole-4-acetic acid, 4(5) imidazolecarboxylic acid, and a variety of other products. The reaction was dependent on the presence of at least catalytic amounts of Fe^{2+} found in highly purified L-histidine and could be completely inhibited in the presence of diethylene triamine pentaactic acid (DTPA).

MATERIALS AND METHODS

Materials

Materials were obtained from the following sources: L-histidine (Fluka, Ultra >99.5%, catalog # 53319, Lot # 1272044 54106207), 50% hydrogen peroxide (EMD, catalog number HX0630-1, lot# 47065720), 70% *tert*-butylhydroperoxide (Sigma, catalog number B-2633, lot # 68H1310), ferrous sulfate heptahydrate (Mallinckrodt, Lot # 1312H26), ethylenediamine tetraacetic acid, EDTA, (Teknova, catalog number E0306, Lot # E030619G501), diethylene triamine pentaacetic acid, DTPA, (TCI America, lot # 0GM01), 4(5)-imidazolecarboxaldehyde (Aldrich, 98% purity, Lot #30402), 2-imidazolecarboxaldehyde (Aldrich, 98% purity, Lot #3 01019JU), histidine methyl ester (Bachem, catalog number E2020, lot number 513104), N-acetyl histidine (M.P. Biochemicals, catalog number 1000092, lot number 7069H), His-Gly (Bachem, catalog number G2305, lot number 510864), Gly-His (Sigma, catalog number G1627, lot number 016K1277), lysine-tyrosine-lysine, KYK, (Sigma, 99% Purity, catalog number L3271, lot number 016K1024), sodium cyanoborohydride (Fluka, catalog number 71435, lot number 1259328 24806204).

Oxidation of L-histidine

Immediately prior to analysis, control solutions of 10 mM L-histidine, 10 mM, 70 mM and 100 mM *tert*-butylhydroperoxide and 100 mM hydrogen peroxide were prepared in 100 mL volumetric flasks, protected from light and stored in an incubator controlled at 37°C unless noted otherwise. The volumetric flasks containing the solutions were gently agitated by hand prior to storage at the desired temperature. Similarly, solutions of *tert*-butylhydroperoxide and hydrogen peroxide at the above concentrations in 10 mM L-histidine were prepared in the same manner as the control solutions. The rate of reaction was monitored by UV absorbance by periodically taking 1 mL aliquots from the volumetric flask and analyzing the sample using a quartz cuvette and a Hewlett Packard 8452A Diode Array Spectrophotometer against a water blank.

Buffer solutions containing 10 mM sodium acetate and 10 mM sodium phosphate adjusted with either hydrochloric acid or sodium hydroxide to pH 3, 5, 6, 7, or 9 were prepared to a final volume of 100 mL in volumetric flasks containing the reactants at 10 mM L-histidine and 100 mM *tert*-butylhydroperoxide to assess the effect of pH on the reaction. The pH 7.0 sample was also prepared in triplicate as described above and evaluated at the additional temperatures of 20, 30, and 40°C. Upon completion of the reaction for all experiments, the UV absorbance was recorded, and this unadjusted UV absorbance of the reactants was subtracted from the UV absorbance obtained after the reaction was allowed to proceed to reveal the absorbance of the products.

To evaluate the effect of metal cations on the reaction, varying amounts of ferrous sulfate heptahydrate from a 0.1 mM stock solution in 10 mM L-histidine prepared immediately prior to these experiments were added to solutions of L-histidine in 10 mL volumetric flasks protected from light with or without 100 mM *tert*-butylhydroperoxide to achieve final concentrations of the metal salt of 0.01 mM, 0.02 mM, and 0.1 mM. The reaction was also conducted in the presence of 0.01, 0.025, 0.050, 0.100, 0.250, and 0.500 mM ethylenediamine tetraacetic acid, EDTA, or in 0.01, 0.025, 0.050, 0.100, 0.250, and 0.500 mM diethylene triamine pentaacetic acid, DTPA, prepared from stock solutions at an initial chelator concentration of 0.5 mM in 10 mM L-histidine. Samples were analyzed using the reversed-phase HPLC method described below.

The Fenton reaction was examined according to the procedure detailed by Stadtman, *et al.* (14) Specifically, a solution of 50 mM L-histidine in 23.5 mM sodium phosphate, pH 7.6 containing 23.5 mM sodium bicarbonate was prepared and allowed to sit for 15 min at room temperature. 100 μM EDTA, from the stock solution of 0.5 mM EDTA described above, was then added and allowed to sit for 5 min, after which 100 μM ferrous sulfate, again from the stock solution described above, was added, followed by the direct addition of either 30 mM hydrogen peroxide or 30 mM *tert*-butylhydroperoxide. The solution was incubated at 37°C for 48 h in a 250 mL volumetric flask protected from light. Analysis of all samples was accomplished by reversed-phase HPLC. Further experiments were conducted to investigate the role of hydroxyl radicals. The hydroxyl radical scavenger, mannitol (34), was weighed and added to the reaction mixture of 10 mM L-histidine and 100 mM tert-butylhydroperoxide in a 10 mL volumetric flask protected from light at a final concentration of 100 mM, and the results were compared directly to control experiments without mannitol.

Purification of the Reaction Products

A Beckman 168 System Gold HPLC was used for all reversed phase liquid chromatography. Absorbance was monitored at 215 nm as well as 260 nm with or without mass spectrometric detection. Unless otherwise specified, an Aquasil C18, 250×2.1 mm, 5 μm, 100 Å column, (Thermo Electron

Corporation) was used. Except for the LC/MS work, where 10 µl was used, 100 µl of the reaction mixture was injected. A gradient of water and methanol at a flow rate of 0.12 mL/min was used for purification of the reaction products. For the first 4 min, the percentage of methanol was maintained isocratically at 10%. At 4 min, the percentage was increased to 25% methanol in 20 min followed by an additional increase to 50% methanol in two and a half minutes. The column then was re-equilibrated at 10% methanol until the end of the 50 min run.

Identification of the Reaction Products

An aliquot, 10 µl, of the reaction mixture was examined via LC/MS by coupling the Beckman 168 System Gold HPLC system to a Thermofinnigan LCQ Deca ESI/Ion trap spectrometer. The Thermofinnigan LCQ Deca ESI Ion Trap mass spectrometer was tuned to the *m/z* of L-histidine in the positive ion mode. The mass spectrometer was set up to analyze the reaction products by MS and MS/MS analysis. The conditions for the mass spectrometer were as follows: Sheath gas flow rate, 20 psi; auxillary gas flow rate, 20 psi; spray voltage, 5.0 kV; capillary temperature, 275.0°C; capillary voltage, 9.00 V; tube lens offset, −15.00 V. For MS/MS fragmentation, the most intense ion was selected, and the normalized collision energy was set at 300.00%, activation energy Q at 0.500, activation time at 300.00 msec, default charge state at 1, isolation width at 2.0*m/z*. The mass range examined was 50 to 500*m/z*.

Spiking experiments were analyzed by reversed phase HPLC analysis. Commercially available 4(5)-imidazolecarboxaldehyde was added to the reaction mixture to help identify the reaction product. The same reversed phase method described previously was used with the exception that mobile phase A was 10 mM potassium phosphate, pH 6.2. A 2 µg solution standard of 4(5)-imidazolecarboxaldehyde was prepared by mixing 25 µl of a 0.1 mg/mL aqueous stock solution with 225 µL of water, and 200 µL were injected onto the column using the reversed phase gradient described above.

To help elucidate the oxidation product of L-histidine, 10 mM L-histidine solution and 100 mM *tert*-butylhydroperoxide in 10 mM sodium phosphate, pH 7.0, were incubated at 45°C. A 1:1 dilution of the reaction mixture with water was prepared. A 125 µL aliquot of the diluted reaction mixture was mixed with 25 µl of the standard solution of 4(5)-imidazolecarboxaldehyde. This mixture was then further diluted with 100 µL of water for a 200 µL injection and analyzed by reversed phase HPLC.

The UV-vis spectra of a 0.05 mM solution of 4(5)-imidazolecarboxaldehyde was measured and compared to a solution of 0.05 mM 2-imidazolecarboxaldehyde. Aliquots, 1 mL, were prepared at a buffer concentration of 0.05 M. 4(5)-imidazolecarboxaldehyde was a pale yellow crystal, which was hydroscopic and readily soluble in water. 2-imidazolecarboxaldehyde was a fine white crystal, which was not significantly hydroscopic, and unlike 4(5)-imidazolecarboxaldehyde, was extremely insoluble in water requiring strongly basic conditions to be soluble. A Hewlett Packard 8452A Diode Array Spectrophotometer and quartz cuvettes were used for UV-vis measurements of 1 mL aliquots. As a comparison, the absorbance of 0.05 mM 4(5) imidazolecarboxaldehyde was measured in 10 mM sodium phosphate, pH 6.9.

Oxidation of L-histidine Analogs

Reactions between *tert*-butylhydroperoxide and either imidazole, histidine methyl ester, N-acetyl histidine, His-Gly, or Gly-His were attempted under similar conditions as described above. Specifically, 10 mM of either imidazole, histidine methyl ester, N-acetyl histidine, the dipeptides of His-Gly and Gly-His were reacted with 100 mM *tert*-butylhydroperoxide in 10 mM sodium phosphate at pH 7.0 and incubated at 37°C in a 100 mL volumetric flask for 17 h. In all cases, control solutions of the individual components were incubated under the same conditions and used to obtain the subtracted UV-vis spectra of the products or analyzed by reversed phase HPLC alongside the reaction mixtures.

Reaction of 4(5) Imidazolecarboxaldehyde with a Tripeptide

A 1 mg/mL solution of tripeptide lysine-tyrosine-lysine, KYK, in 10 mM sodium phosphate, pH 6.9 was prepared. L-histidine or 4(5) imidazolecarboxaldehyde was added to the solution containing the KYK at a final concentration of 1 mg/mL in 1:1, 1:2, and 1:3 ratios to KYK. These experiments were performed in both the absence and presence of 10 mg/mL sodium cyanoborohydride. All samples were incubated at 37°C for 1 h. The samples were then analyzed by LC/MS using a Beckman HPLC coupled with a Thermofinnigan LCQ Deca ESI-ion trap mass spectrometer and a Polaris C18-ether 250× 2.1 mm column (Varian, part number A2020250X020, serial number 1000815) with a simple gradient between mobile phase A, 0.1% trifluoroacetic acid and mobile phase B, 90% acetonitrile with 0.085% trifluoroacetic acid.

RESULTS

Oxidation of L-histidine

Initial experiments were conducted to investigate the potential of free L-histidine to oxidize under conditions that

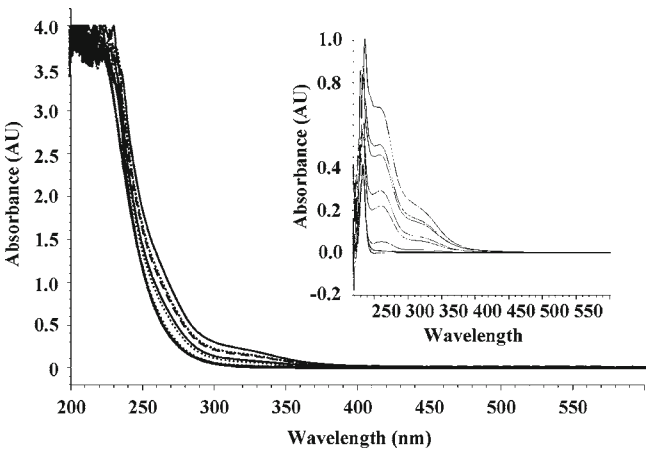

Fig. 1. Monitoring the reaction between 100 mM *tert*-butylhydroperoxide and 10 mM L-histidine in 10 mM sodium phosphate, pH 6.9, by UV-vis spectroscopy over 1, 2, 3, 7, 20, 27, 44, 51, and 78.5 h storage at 37°C resulted in an increase in absorbance at approximately 260 nm and 320 nm. The insert shows the growth of the reaction products after subtracting the spectra of the 100 mM *tert*-butylhydroperoxide reactant over the same 78.5 h period.

exclude the addition of metals or light. It was observed that in the presence of *tert*-butylhydroperoxide the UV-spectrum changed and produced spectrum with apparent maxima at 260 and 320 nm (Fig. 1). The absorbance increase was not observed when individual components of the reaction were incubated under similar conditions. From the UV spectrum, it was observed that the product from this reaction has apparent maxima at 260 nm with the peak intensity being less at 320 nm; therefore, all future experiments were monitored at 260 nm. Hydrogen peroxide was also tested but found to be less reactive such that the organic peroxide, *tert*-butylhydroperoxide, produced significantly more of the unknown product with an absorbance maxima of 260 nm (data not shown). The reaction was dependent upon both the concentration of *tert*-butylhydroperoxide and pH with higher concentrations of *tert*-butylhydroperoxide resulting in more of the product. The reaction proceeded rapidly at pH 6 and above with little or no reaction observed at pH 5 and below (Fig. 2). An increase in the rate of product formation by the reaction was seen as the temperature was increased from 20 to 40°C (data not shown).

Purification of the Reaction Products

In an effort to purify the product from the reactants, a reversed phase HPLC method was developed, which allowed the main products to be monitored by LC/MS. The UV spectrum of the product at 13 min (peak #5) was the only peak with an absorbance maxima at 260 nm, identical to that of the incubated sample in Fig. 1 with an absorbance maximum at 260 nm (Fig. 3).

Identification of the Reaction Products

The products of the reaction with *tert*-butylhydroperoxide and L-histidine that were separated by reversed phase HPLC (Fig. 3) were analyzed by mass spectrometry. For ease of identification, the masses were designated as peaks 1 to 5

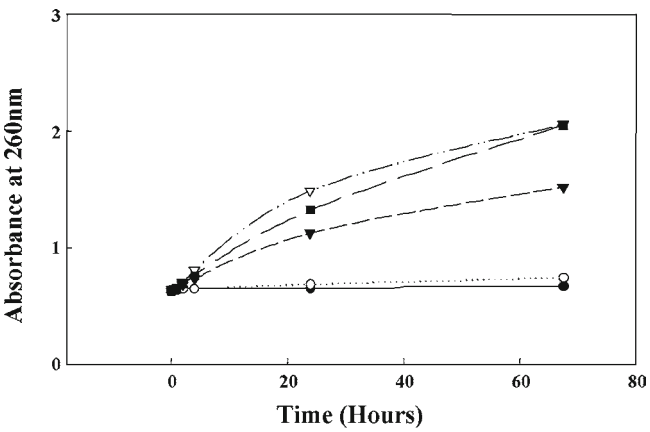

Fig. 2. The reaction between 100 mM *tert*-butylhydroperoxide and 10 mM L-histidine was monitored with respect to pH. The reactants were placed into 10 mM sodium acetate, 10 mM sodium phosphate buffer that was adjusted throughout the pH range of 3.0 to 9.0. The absorbance was monitored over time using a Hewlett Packard 8452A Diode Array Spectrophotometer. Data is unsubtracted. (key: —●— pH 3.0, · · ·○· · · pH 5.0, —▼— pH 6.0, —■— pH 7.0 —▽· · · pH 9.0).

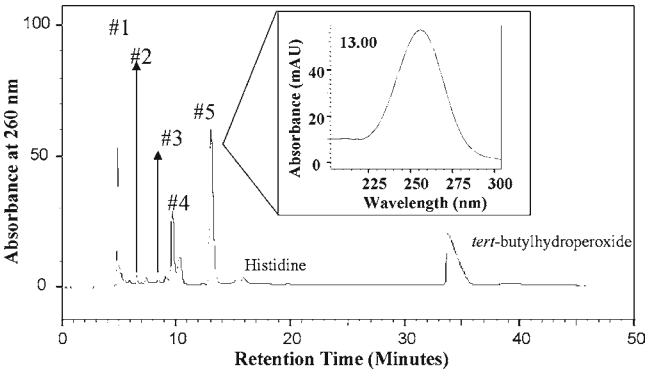

Fig. 3. Reversed phase HPLC of *tert*-butylhydroperoxide and L-histidine reaction products. The identified peaks have been labeled 1 to 5 for reference. Peak #5 has an absorbance maximum at 260 nm.

and found to have *m/z* ratios of 184.2, 127.1, 113.1, 168.2, and 97.2. The MS/MS of peak #1 having the (M+H) ion of 184.2 yielded *m/z* ratios of 156.1, 137.9, and 110.1. The *m/z* ratio of 156.1 represents a loss of 28.1 and corresponds to the neutral loss of carbon monoxide to yield the mass of L-histidine. The *m/z* ratio of 137.9 corresponds to the subsequent neutral loss of water from the parent ion with m/z of 156.1. Finally, a successive neutral loss of an additional carbon monoxide results in the peak at *m/z* 110.1. For peak #2, having a $[M+H]^+$ of 127.1, the loss of 46.1 results in an m/z ratio of 81.0, which can be attributed to the neutral losses of water and carbon monoxide from a carboxylic acid functional group on the precursor ion. This is consistent with imidazole-4-acetic acid. Peak #3 has an *m/z* ratio of 113.1, which upon fragmentation loses 45.1, consistent with the neutral losses of carbon monoxide and ammonia. For peak #4, which has an $[M+H]^+$ of 168.2, the MS/MS fragmentation produced ions having the *m/z* ratio of 124.1, 107.0, and 95.1. The loss of 44.1 is due to the loss of a carbon dioxide (CO_2). The fragment having a *m/z* ratio of 107.0 may represent the additional loss of ammonia from the product with an *m/z* ratio of 124.1. The *m/z* loss resulting in the fragmentation product with an *m/z* ratio of 95.1 can not be definitively assigned at this time. Peak #5 has an *m/z* of 97.1 with the MS/MS spectrum showing a single ion with an *m/z* ratio of 69.6 amu corresponding to a loss of 27.6 from the $[M+H]^+$ ion. These masses match those expected for the intact imidazole ring and the neutral loss of carbon monoxide. Based on this analysis, a likely candidate for this unknown product was 4(5)-imidazolecarboxaldehyde that also has a molecular mass of 97.2 and an *m/z* of 69.0 upon fragmentation (Fig. 4) matching that observed for peak #5. Identification of the product was further confirmed by adding the 4(5)-imidazolecarboxaldehyde standard directly to the reaction mixture of L-histidine and *tert*-butylhydroperoxide followed by analysis by reverse phase HPLC (Fig. 5). Both the 4(5)-imidazolecarboxaldehyde standard and the product of the reaction mixture had identical retention times of 11.8 min with peak heights of 700 mAu and 200 mAu, respectively. The reaction mixture containing the spiked 4(5)-imidazolecarboxaldehyde standard also showed a single peak with a retention time of 11.8 min and a peak height of 900 mAu, which was equal to the sum of the combined peak heights for the standard and the sample.

4(5)-imidazolecarboxaldehyde has the same mass as 2-imidazolecarboxaldehyde, making it difficult to differentiate

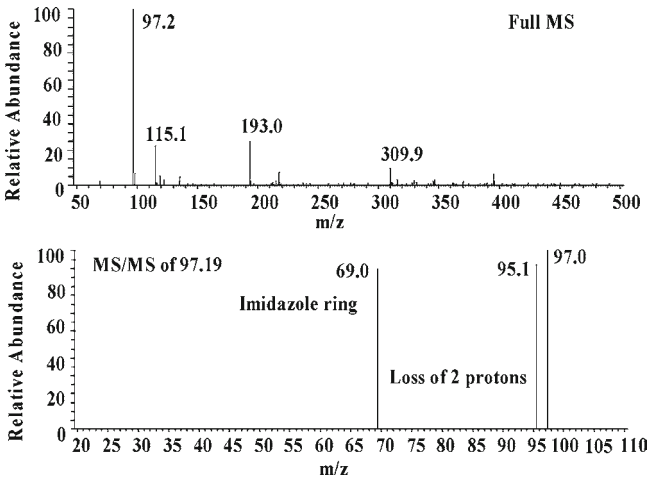

Fig. 4. Mass spectroscopic analysis of 10 mM 4(5)-imidazolecarboxaldehyde in water showed the expected mass and a similar MS/MS spectrum as that of the reaction product of L-histidine and *tert*-butylhydroperoxide.

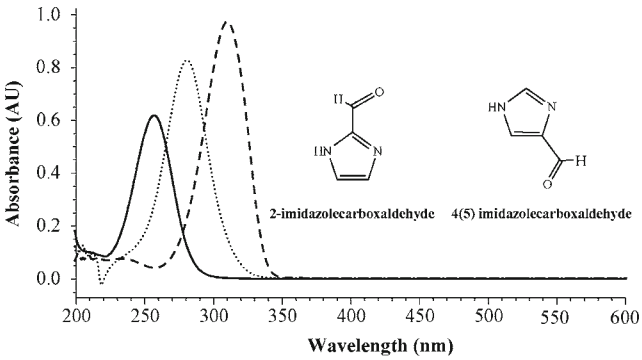

Fig. 6. Both 4(5)-imidazolecarboxaldehyde and 2-imidazolecarboxaldehyde have the same MS spectrum and fragmentation pattern; therefore, both could be the product. A comparison of the UV-vis absorbance at pH 13 revealed that — — — 2-imidazolecarboxaldehyde has an absorbance maximum at approximately 320 nm while ••••••••• 4(5)-imidazolecarboxaldehyde has an absorbance maximum at 275 nm. As a comparison, ——— 4(5)-imidazolecarboxaldehyde has an absorbance maximum at 260 nm in 10 mM sodium phosphate at pH 6.9.

between the two structures based only on the MS and RP-HPLC data. Interestingly, 2-imidazolecarboxaldehyde is soluble around pH 13 but extremely insoluble at low pH. The UV spectrum of 2-imidazolecarboxaldehyde has an absorbance maximum at approximately 320 nm, distinctly different from 4(5)-imidazolecarboxaldehyde that has an absorbance maximum at 280 nm at pH 13 in 10 mM sodium phosphate / NaOH buffer (Fig. 6). For comparison, 4(5) imidazolecarboxaldehyde has an absorbance maximum of 260 nm at pH 6.9 in 10 mM sodium phosphate. The absorbance maximum of the 4(5)-imidazolecarboxaldehyde is the same as that for the reaction product between L-histidine and *tert*-butylhydroperoxide (Figs. 1 and 3), further confirming the identity of the reaction product under investigation.

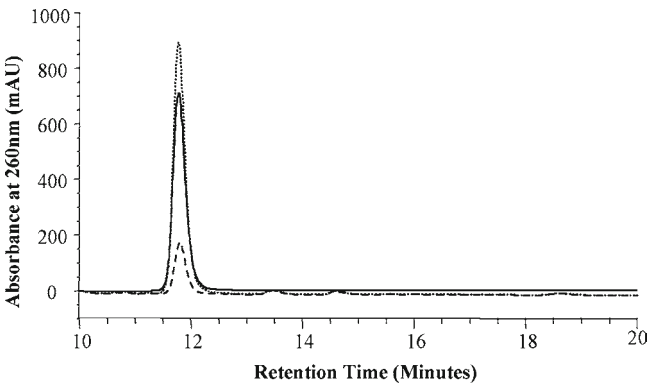

Fig. 5. A Spiking experiment of 4(5)-imidazolecarboxaldehyde with the product from the reaction between L-histidine and *tert*-butylhydroperoxide was conducted. A standard solution of ——— 4(5)-imidazolecarboxaldehyde was prepared, and 2 µg was loaded on the column. The reaction mixture — — — of 10 mM L-histidine and 100 mM *tert*-butylhydroperoxide in 10 mM Sodium Phosphate, pH 7.0 was incubated at 45°C and subsequently loaded on the column by taking 125 µl of the sample and diluting it with 125 µL of water and then injecting 200 µL of the resulting solution. A 25 µL aliquot of the 4(5)-imidazolecarboxaldehyde solution was spiked with 125 µL of the reaction mixture and then the solution was further diluted with 100 µL of water. A 200 µL aliquot of the resulting spiked solution ••••••••• was injected on the column.

Proton NMR experiments were conducted on samples resuspended in deuterated water using a 600 MHz NMR with a cryoprobe (data not shown). The following chemical shifts were observed for the peak having a mass of 97.1 *m/z*: a singlet at 9.7 ppm typically assigned to the proton of an aldehyde, singlets at 8.1 and 7.9 which correspond to the two protons of the imidazole ring. These observations were consistent with the expected chemical shifts for 4(5)-imidazolecarboxaldehyde.

Role of Metal Cations

The role of metal cations in the reaction was also monitored by reversed phase HPLC. As seen in Figs. 7 and 8, the reaction of L-histidine with *tert*-butylhydroperoxide produced a variety of reaction products with different UV spectrum. The peak with unique absorbance spectra relating to absorbance maxima at 260 nm, labeled as peak #5 in Fig. 8, elutes at either 11.5 or 13.5 min, depending upon whether the HPLC system or the LC/MS system was used for detection. The impact that metal cations have on this reaction system was examined using the metal chelator ethylenediamine

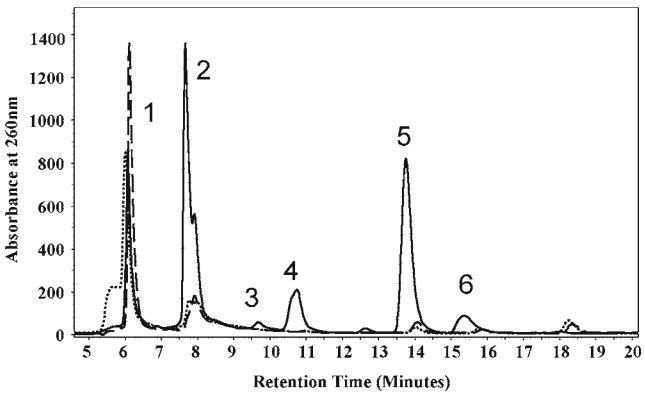

Fig. 7. The reaction between 10 mM L-histidine and 100 mM *tert*-butylhydroperoxide in 10 mM sodium phosphate, pH 7.0, was monitored by reverse phase HPLC ——— and compared to reactions containing 0.01 mM EDTA — — or 0.01 mM DTPA ••••••••• after incubation at 37°C for 1 day.

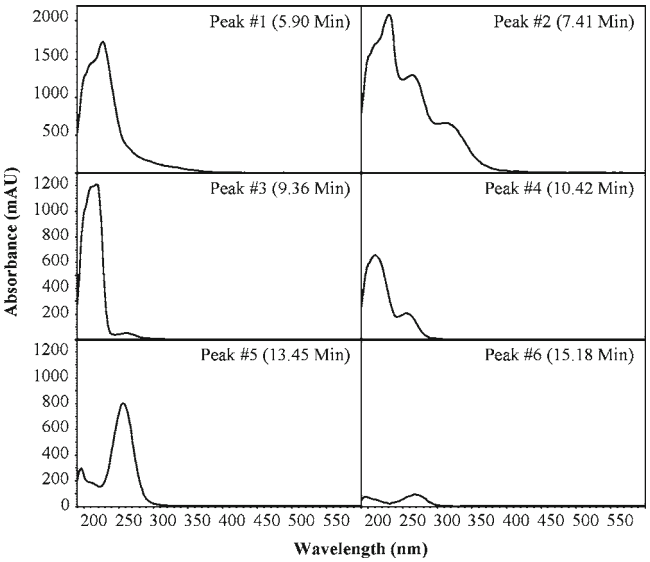

Fig. 8. The individual peak absorption spectra for the reaction between 10 mM L-histidine and 100 mM *tert*-butylhydroperoxide in 10 mM sodium phosphate, pH 7.0, was monitored by reversed phase HPLC after incubation at 37°C for 1 day.

tetraacetic acid (EDTA) to sequester any metal ions that were present. Since EDTA is known to form oxygen active metal complexes to produce reactive oxygen species (ROS), additional experiments were conducted using diethylene triamine pentaacetic acid (DTPA), which irreversibly binds metal cations and does not form reactive complexes (35,36). It was observed that in the presence of either chelator, the reaction failed to proceed for 24 h at 37°C, while control experiments without a chelator resulted in degraded L-histidine. A control experiment in which DTPA was added to a final concentration of 1 mM after the reaction mixture with 10 mM L-histidine and 100 mM *tert*-butylhydroperoxide was allowed to proceed at 37°C for 24 h showed the formation of the product (data not shown). Interestingly, the addition of Fe (II), as $FeSO_4$, to L-histidine alone in the absence of added peroxides resulted in significant degradation of L-histidine (Fig. 9), principally to a single peak with an absorbance maximum of 260 nm, similar to that observed from peak #5 in Fig. 8. Increasing the amount of $FeSO_4$ within the range of 0.01 mM, 0.02 mM, and 0.1 mM resulted in additional oxidation of L-histidine.

The similarities of the reaction system to well-known Fenton chemistry led us to suspect that a similar reaction was taking place, and we therefore investigated the role of hydroxyl radicals using the Fenton reaction system as described in the materials and methods section. The reactions using either hydrogen peroxide or *tert*-butylhydroperoxide both produced chromatograms with a peak having similar retention times, between 11 and 12 min, and absorbance maximum at 260 nm (data not shown) similar to the reaction of *tert*-butylhydroperoxide with L-histidine alone (Fig. 7). Differences exist, though, in the number and quantity of products produced from the reactions with the two peroxides. Additionally, the complete reaction profiles contain a variety of other products having different retention times than those observed for the simple reaction between L-histidine and *tert*-butylhydroperoxide. The reaction profiles also differ between the reactions with the organic peroxide and hydrogen peroxide. Addition of 100 mM mannitol, a hydroxyl radical scavenger, resulted in a small decrease in the formation of the peak having an absorbance maximum of 260 nm, but the overall result was that mannitol still allowed the reaction to proceed to the same products, albeit at a slower rate. In the absence of EDTA, the reaction proceeds at a much faster rate. Bicarbonate ion dependence of the Fenton chemistry has been reported in the literature (14). The reaction under investigation here demonstrated a lack of dependence on the presence of bicarbonate ion.

Oxidation of L-histidine Analogs

To determine the potential impact of this reaction on proteins, model compounds were selected based on their chemical structure. Imidazole, L-histidine methyl ester (Fig. 10), N-acetyl histidine as well as the dipeptides His-Gly

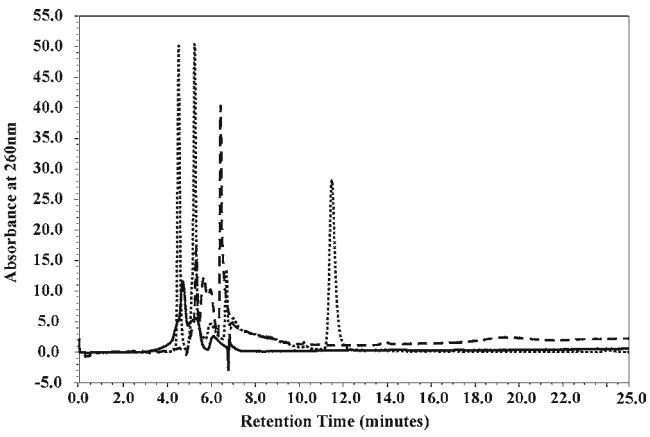

Fig. 9. The reaction between 10 mM L-histidine and 0.1 mM ferrous sulfate in 10 mM sodium phosphate, pH 7.0, was monitored by reversed phase HPLC ····· after 2 days of incubation at 37°C and compared to incubation of the individual components of 10 mM L-histidine ——— and 0.1 mM ferrous sulfate — — during the same time period.

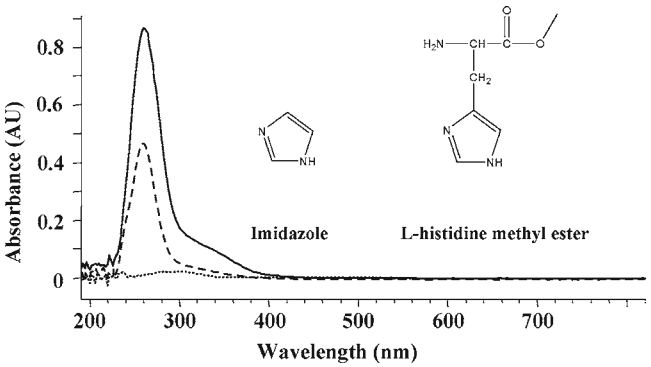

Fig. 10. To investigate the potential for this reaction to damage proteins, 10 mM imidazole was incubated with 100 mM *tert*-butylhydroperoxide in 10 mM sodium phosphate at pH 7.0. No reaction was observed. Conversion of the carboxylic acid functional group to a methyl ester, however, did not inhibit the reaction. The imidazole reaction mixture is depicted as follows ·····, the reaction of L-histidine methyl ester is represented by — — —, and the control reaction of free L-histidine with *tert*-butylhydroperoxide is shown by ———.

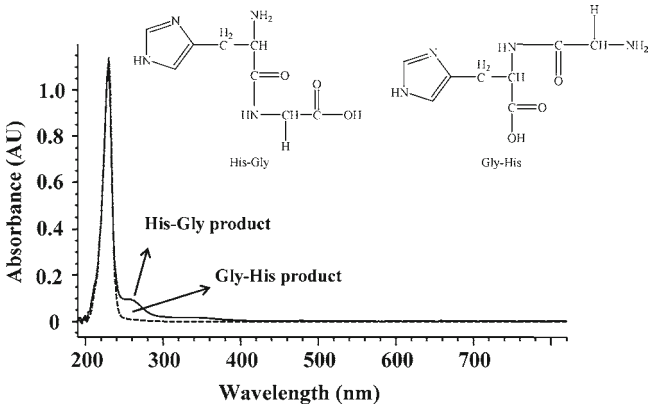

Fig. 11. His-Gly and Gly-His dipeptides were incubated with *tert*-butylhydroperoxide in an effort to investigate the mechanism of reaction. The dipeptide of His-Gly — — — reacted with *tert*-butylhydroperoxide while Gly-His ——— did not. The reaction was carried out using 10 mM of the respective dipeptide and 100 mM *tert*-butylhydroperoxide in 10 mM sodium phosphate, pH 7.0, and incubated at 37°C for 17 h.

and Gly-His (Fig. 11) were examined. Individually, each of these model compounds was incubated with 100 mM *tert*-butylhydroperoxide at 37°C in 10 mM Sodium Phosphate, pH 7.0. The rate of reaction was monitored by UV-vis absorbance at 260 nm. It was observed that imidazole and N-acetyl histidine did not react with *tert*-butylhydroperoxide (data not shown), while histidine methyl ester was able to form a product with an absorbance maximum of 260 nm as observed by UV-vis absorbance. The reaction between His-Gly also proceeded to a product with an absorbance maximum of 260 nm, while the dipeptide Gly-His was unreactive (Fig. 11). Interestingly, His-Gly formed 4(5)-imidazolecarboxaldehyde at a faster rate than L-histidine alone followed by histidine methyl ester producing the least amount during the same amount of time (Fig. 12).

Reaction of 4(5) Imidazolecarboxaldehyde with a Tripeptide

Aldehydes have the potential to form a Schiff base with the primary amines of a peptide or protein leading to chemical modifications of that peptide or protein. Generally, the reaction proceeds through the formation of an imine bond from the combination of the aldehyde and the primary amine. This bond is easily reduced to a secondary amine by the addition of sodium cyanoborohydride. To confirm that 4(5) imidazolecarboxaldehyde demonstrates this propensity to form a Schiff base with primary amines, it was incubated with the model peptide, KYK. Characterization of the reaction mixture by LC/MS after incubation at 37°C for 1 h produced the expected mass of 438.2*m/z*. Upon incubation of KYK with cyanoborohydride, only one peak was observed having the same mass. However, upon the addition of 4(5) imidazolecarboxaldehyde with KYK, a new peak having a mass of 516.3*m/z* was observed. Addition of cyanoborohydride to the reaction of KYK with 4(5) imidazolecarboxaldehyde resulted in a product with an *m/z* of 518.5. Further, investigating the ratio of KYK to 4(5) imidazolecarboxaldehyde by increasing the aldehyde from 1x, 2x, and 3x, the concentration of KYK resulted in products with *m/z* of 518.4, 598.4, and 678.4, respectively (data not shown).

DISCUSSION

The studies presented here originated from an initial observation in our labs during liquid protein formulation stability studies with histidine-based buffer systems. We found that while monitoring placebo samples over time by size-exclusion chromatography, the excipient peak appeared to increase over time with some but not all formulation preparations. Eventually, it was determined that the increase in absorbance was due to the presence of histidine and polysorbate, which together produced a product with a unique UV spectrum similar to that shown in Fig. 1. It was suspected that peroxides from the degradation of the Polysorbate (51,52) were reacting with the histidine to produce the absorbing species. In order to reproduce the system in a more defined manner and study conditions leading to the degradation product(s), we set up a model system using free L-histidine with either *tert*-butylhydroperoxide or hydrogen peroxide. We found that despite using >99.5% pure L-histidine, free L-histidine in the presence of the peroxides was susceptible to oxidation in the absence of either added metal cations or exposure to light. Based on UV spectroscopic analysis, the new species was likely to be 4(5)-imidazolecarboxaldehyde, which has not previously been reported in the literature as an oxidation product of L-histidine following reaction with *tert*-butylhydroperoxide or hydrogen peroxide. This identification was confirmed by mass spectrometry analysis (MS and MS/MS), proton NMR and RP HPLC. The only other report in the literature we are aware of is by Gewitz *et al.* (37), who reacted free L-histidine with L-amino acid oxidase and horseradish peroxidase to yield 4(5)-imidazolecarboxaldehyde, 4(5)-imidazolecarboxylic acid, carbon dioxide, ammonia, and hydrogen peroxide. 4(5)-imidazolecarboxaldehyde is commercially available and can be prepared through a variety of synthetic pathways (37–49), which are different from the oxidation of L-histidine currently being discussed.

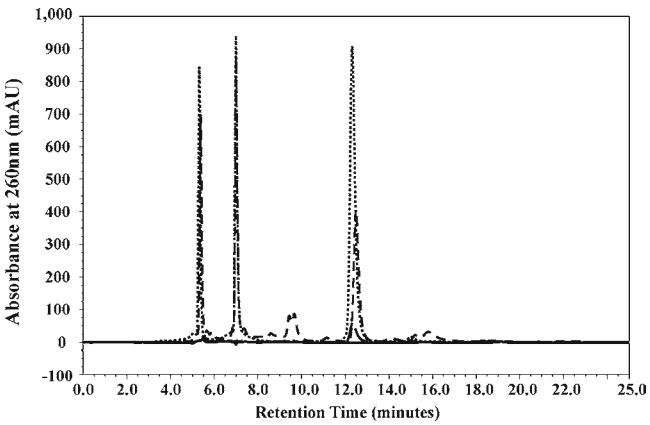

Fig. 12. The reaction between 10 mM L-histidine and 100 mM *tert*-butylhydroperoxide in 10 mM Sodium Phosphate, pH 7.0, was monitored by reverse phase HPLC — · — and compared to similar reactions between 10 mM His-Gly ····· and 100 mM tert-butylhydroperoxide and to 10 mM L-histidine methyl ester with 100 mM *tert*-butylhydroperoxide — — — after incubation at 37°C for 2 days. 100 mM *tert*-butylhydroperoxide ——— incubated under the same conditions.

Formation of the product was found to depend on a number of factors, including pH, temperature, metal content and availability of functional groups on the histidine. Additionally, we also found that iron added in the form of ferrous sulfate increased the formation of the 4(5)-imidazolecarboxaldehyde, demonstrating that this was also part of the reaction mechanism. In retrospect, this makes sense, since commercially available high purity L-histidine contains some amount of contaminating metal ions. Addition of EDTA to the L-histidine buffer prevented formation of the 4(5)-imidazolecarboxaldehyde. Inconsistency in metal ion content in the L-histidine buffer, along with low level metal contamination from the buffer preparation process, may also explain the variability of the peak observed at 280 nm during SEC analysis of the placebo. The pH dependence on the rate of reaction suggested that the imidazole ring must be deprotonated for the reaction to occur. Likely, the imidazole ring needs to be deprotonated to effectively bind the trace levels of metal in solution and allow the reaction to proceed (50). Alternatively, the deprotonated imidazole ring may help stabilize a reaction intermediate. While it is possible the primary amine of L-histidine is involved in the binding of the metal, this does not seem to correlate with the pH dependence of the reaction, as the primary amine is expected to be protonated and not likely to effectively bind metal cations.

The similarity in the reaction rates between pH 7 and 9 also suggests that deprotonation of the amine is not a rate-limiting step in the reaction. While the pKa of the amino group did not appear important, the presence of the amine was important for the reaction to proceed as evidenced by the lack of reaction between either the Gly-His dipeptide, imidazole or N-acetyl L-histidine with the organic peroxide. This is in contrast to the photooxidation of L-histidine, which is independent of protecting groups at the primary amine or carboxylic acid functional groups (8). Based on the reaction of the His-Gly dipeptide and histidine methyl ester with the *tert*-butylhydroperoxide, the carboxylic moiety on the L-histidine was not deemed important for the reaction. However, it is interesting to note that the relative rate of the reaction for His-Gly is higher than L-histidine, which in turn is higher than that observed for histidine methyl ester; therefore, while blocking the carboxylic acid functional group does not impair the reaction, it appears to play a role in the rate of the reaction.

Fenton chemistry produces 4(5)-imidazolecarboxaldehyde, as was confirmed by spiking experiments, but also produces a variety of other products that are distinctly different than those observed by L-histidine and *tert*-butylhydroperoxide alone. Close examination of the Fenton system showed no inhibition of the reaction in the presence of the hydroxyl radical scavenger mannitol. While it has been noted previously, hydroxyl radical scavengers may not inhibit Fenton chemistry, since the Fenton reaction is likely to proceed via a "caged process," the current system is also not inhibited by iron concentrations in the range of 10–100 μm, which has been reported as inhibitory for amino acid oxidation via Fenton chemistry (14). Further, the presence or absence of bicarbonate ion had little effect on the current reaction, arguing against the role of hydroxyl radicals in the current reaction.

In addition to its possible interaction with the imidazole ring, iron is also expected to be involved with formation of radical intermediates of the *tert*-butylhydroperoxide. Fossey *et al*. report that in the presence of Fe^{2+}, *tert*-butylhydroperoxide forms a *t*-BuO radical (53). More recently, Guo *et al*. reported that the same reaction between Fe^{2+} and *tert*-butylhydroperoxide resulted in the formation of methoxyl radicals (54). Either of these radicals would be expected to react with the histidine, forming a variety of oxidation products. This is consistent with the wide array of products delineated in the reactions described here. The complexity of the radical-mediated reactions also makes it difficult to definitively assign structures to the observed oxidation products and hence derive a reaction mechanism. Further experiments are underway to identify reaction intermediates, reaction kinetics and mass balance of the reactants and products and will be the subject of a future paper.

The data demonstrate that even pure L-histidine contains catalytic amounts of metal cations that allow L-histidine to degrade at elevated temperatures near physiological pH leading to the formation of 4(5) imidazolecarboxaldehyde. Aldehydes are commonly known to form Schiff bases with primary amines; therefore, it was reasonable to expect that 4(5)-imidazolecarboxaldehyde has the potential to attack the primary amines of proteins when histidine is used as a buffer during protein formulation. It has been pointed out that aldehydes will even form Schiff bases with the primary amine of free L-histidine (23). In fact, it was observed that 4(5) imidazolecarboxaldehyde was indeed able to form a Schiff base with the primary amines of a tripeptide. The addition was observed to be stoichiometric, with all three primary amines reacting upon the addition of a 3-fold excess of the aldehyde. The importance of this in a liquid formulation of a protein is that formation of the 4(5) imidazolecarboxaldehyde could result in modification of the protein at the primary amines found at the amino terminus and on Lys residues. This assertion is in agreement with our early observations that the growth of the 280 nm excipient peak was suppressed in protein-containing samples.

CONCLUSION

In liquid protein formulations, the stability of the buffer should be considered, since the buffer can potentially oxidize. While instability in the presence of light is known, it was assumed that storage in the dark would prevent degradation of the L-histidine. In fact, this was not true such that degradation of L-histidine by *tert*-butylhydroperoxide was observed with a major product of the reaction being 4(5)-imidazolecarboxaldehyde, which has not been fully studied in the literature as an oxidation product of L-histidine. Despite using high purity L-histidine, trace metal contaminants lead to the oxidation of L-histidine that could be prevented by the presence of metal chelators such as EDTA. It would also be expected that the presence of surfactants would increase the rate of reaction, as they are known to produce organic peroxides (51,52). Carbonyl compounds are known to reversibly form Schiff bases with amines, thereby altering the chemical properties of both the amine and the carbonyl compound. It is reasonable to believe that the product from the reaction of L-histidine and peroxides, 4(5)-imidazolecarboxaldehyde, would form Schiff bases with the primary amine of the N-terminus of a protein and with that of lysine resulting in chemical modification of the protein. In addition to the degradation of free histidine, it may also be possible for the N-terminal histidine residue of a protein to degrade in a similar manner. The presence of a N-terminal histidyl group would provide the necessary primary

amine for the reaction to proceed as shown for the dipeptide His-Gly, resulting in the loss of the N-terminal histidyl residue from the protein. Together, these data suggest that it is important not only to understand the degradation pathways of proteins but also the buffers when developing liquid formulations for protein solutions.

ACKNOWLEDGEMENTS

The authors would like to thank Carey Brennar and Dr. Scott Buckel for initially asking what the new peak was observed by SE HPLC and Drew Nichols for his initial work limiting some of the possibilities. We also would like to thank Dr. Songpon Deechongkit and Dr. David Hambly for many thoughtful discussions, Tsang-Lin Hwang for NMR analysis and Dr. Mike Treuheit for critical reading of the manuscript.

REFERENCES

1. Chen B, Bautista R, Yu K, Zapata GA, Mulkerrin MG, Chamow SM. Influence of histidine on the stability and physical properties of a fully human antibody in aqueous and solid forms. Pharm Res. 2003;20(12):1952–60.
2. Miskoski S, Garcia NA. Influence of the peptide bond on the singlet molecular oxygen-mediated (O2[delta g]) photooxidation of histidine and methionini depeptides. A kinetic Study. Photoch Photobiol. 1993;57(3):447–52.
3. Wasserman HH, Wolff MS, Stiller K. The dye-sensitized photooxidation of imidazoles—trapping of intermediates by nucleophiles. Tetrahedron. 1980;37(1):191–200.
4. Iesce MR, Cermola F, Temussi F. Photooxygenation of heterocycles. Curr Org Chem. 2005;9(2):109–39.
5. George MV, Bhat B. Photooxygenation of nitrogen heterocycles. Chem Rev. 1979;79(5):447–78.
6. Davies MJ, Truscott RJW. Photo-oxidation of proteins and its role in cataractogenesis. J Photochem Photobiol B: Biol. 2001;63:114–25.
7. Kang P, Foote CS. Photosensitized oxidation of 13C, 15N-labeled imidazole derivatives. J Am Chem Soc. 2002;124 (32):9629–38.
8. Tomita M, Irie M, Ukita T. Sensitized photooxidation of histidine and its derivatives. Products and mechanism of the reaction. Biochemistry. 1969;8(12):5149–60.
9. Dakin HD. The oxidation of amido-acids with the production of substances of biological importance. J Biol Chem. 1906;1(2):171–6.
10. Dakin HD. The formation of glyoxylic acid. J Biol Chem. 1906;1 (4):271–8.
11. Dakin HD. The Oxidation of Leucin, α-amido-isovaleric acid and of α-amido-*n*-valeric acid with hydrogen peroxide. The J Biol Chem. 1908;4(1):63–76.
12. Amici A, Levine RL, Tsai L, Stadtman ER. Conversion of amino acid residues in proteins and amino acid homopolymers to carbonyl derivatives by metal-catalyzed oxidation reactions. J Biol Chem. 1989;264(6):3341–6.
13. Stadtman ER. Oxidation of free amino acids and amino acid residues in proteins by radioylsis and by metal-catalyzed reactions. Ann Rev Biochem. 1993;62:797–821.
14. Stadtman ER, Berlett BS. Fenton chemistry. Amino acid oxidation. J Biol Chem. 1991;266(26):17201–11.
15. Uchida K, Kawakishi S. Identification of oxidized histidine generated at the active site of Cu, Zn-superoxide dismutase exposed to H2O2. Selective generation of 2- oxo-histidine at the histidine 118. J Biol Chem. 1994;269(4):2405–10.
16. Schoneich C. Mechanism of Metal-catalyzed oxidation of histidine to 2-oxo-histidine in peptides and proteins. J Pharm Biomed Anal. 2000;21:1093–7.
17. Gangopadhyay S, Ali M, Banerjee P. Kinetics and Mechanism of the Oxidation of Histidine by Dodecatungstocobaltate (III) and trans-Cyclohexane-1, 2-diamine-N, N, N′, N′-tetraacetatomanganate(III) in Aqueous Medium. J Chem Soc Perkin Trans. 1992;2 (5):781–5.
18. Laloo D, Mahanti MK. Kinetics of oxidation of amino acids by alkaline hexacyanoferrate (III). J Chem Soc Dalt Trans. 1990;1990(1):311–3.
19. Hureiki L, Croue JP, Legube B. Chlorination studies of free and combined amino acids. Water Res. 1994;28(12):2521–31.
20. Pereira WE, Hoyano Y, Summons RE, Bacon VA, Duffield AM. Chlorination Studies II. The reaction of aqueous hypochlorous acid with α-amino acids and dipeptides. Biochim Biophys Acta. 1973;313:170–80.
21. Rangappa KS, Chandraju S, Gowda NMM. Manganese(III) oxidation of L-Lysine and L-Histidine in pyrophosphate solution: a kinetic and mechanistic study. Synth React Inorg Met-Org Chem. 1998;28(2):275–94.
22. Pinto I, Sherigara BS, Udupa HVK. Electrolytically generated manganese(III) sulfate for the oxidation of L-Histidine in aquoeous sulfuric acid: a kinetic study. Bull Chem Soc Jpn. 1990;63:3625–31.
23. Yong SH, Karel M. Reaction of histidine with methyl linoleate: characterization of the histidine degradation products. J Amer Oil Chem Soc. 1978;55:352–7.
24. Karim E, Mahanti MK. Kinetics of oxidation of amino acids by quinolinium dichromate. Pol J Chem. 1992;66:1471–6.
25. Satyanarayana MV, Sundar BS, Murti PSR. Kinetics and mechanism of oxidation of a few α-amino acids by trichloroisocyanuric acid. Oxid Comm. 1993;16(4):364–72.
26. Jones MN. Surfactants in membrane solubilisation. Int J Pharm. 1999;177:137–59.
27. Sivars U, Tjerneld F. Mechanisms of phase behaviour and protein partitioning in detergent/polymer aqueous two-phase systems for purification of integral membrane proteins. Biochim Biophys Acta. 2000;1474:133–46.
28. Ha E, Wang W, Wang YJ. Peroxide formation in polysorbate 80 and protein stability. J Pharm Sci. 2002;91(10):2252–64.
29. Cleland JL, Powell MF, Shire SJ. The development of stable protein formulations: a close look at protein aggregation, deamidation, and oxidation. Crit Rev Ther Drug Car Sys. 1993;10(4):307–77.
30. Carpenter JF, Pikal MJ, Chang BS, Randolph TW. Rational design of stable lyophilized protein formulations: some practical advice. Pharm Res. 1997;14(8):969–75.
31. Kappelgaard A-M. Liquid growth hormone: perservatives and buffers. Horm Res. 2004;62(S 3):98–103.
32. Katayama DS, Nayar R, Chou DK, Valente JJ, Cooper J, Henry CS, *et al.* Effect of buffer species on the thermally induced aggregation of interferon-tau. J Pharm Sci. 2006;95(6):1212–26.
33. Barnard ML, Gurdian S, Diep D, Ladd M, Turrens JF. Protein and amino acid oxidation is associated with increased chemiluminescence. Arch Biochem Biophys. 1993;300(2):651–6.
34. Auerbach PSN, Robert L. Harrison's principles of internal medicine. 17th ed.: McGraw-Hill, 2008. p 2747.
35. Bertrand R, Capony J-P, Derancourt J, Kassab R. Detection of nucleotide- and F-actin induced movements in the switch II Helix of the skeletal myosin using its differential oxidative mediated by an iron-EDTA complex disulfide-linked to the strong actin binding site. Biochemistry. 1999;38:11914–25.
36. McCord JM, Day Jr ED. Superoxide-dependent production of hydroxyl radical catalyzed by iron-EDTA complex. FEBS Lett. 1978;86(1):139–42.
37. Gewitz H-S, Piefke J, Langowska K, Vennesland B. The formation of hydrogen cyanide from histidine in the presence of amino acid oxidase and peroxidase. Biochim Biophys Acta (BBA) Enzymol. 1980;611(1):11–26.
38. Ahond A, Mourabit AA, Bedoya-Zurita M, Heng R, Braga RM, Poupat C, *et al.* Synthese stereoselective de la girolline. Tetrahedron. 1992;48(21):4327–46.
39. Aulaskari P, Ahlgren M, Rouvinen J, Vainiotalo P. Preparation and structure determination of 1-Benzyl-, 1-Methyl- and 1H-5-[(2-Nitro-2-Phenyl)ethenyl)imidazoles. J Heterocycl Chem. 1996;33:1345–54.
40. Kim J-W, Abdelaal SM, Bauer L, Heimer NE. Synthesis of 1-(Dimethylsulfamoyl)-2- and 5-Imidazolecarboxaldehydes. Rearrangement of 1-(Dimethylsulfamoyl)-5-imidazolecarboxaldehyde to the 4-Carboxaldehyde [1]. J Heterocycl Chem. 1995;32:611–20.

41. Kirk KL. 4-Lithio-l-tritylimidazole as a synthetic intermediate. Synthesis of imidazole-4-carboxaldehyde. J Heterocycl Chem. 1985;22:57–9.
42. Lindgren G, Stensio K-E, Wahlberg K. Synthesis and photocyclization of some 4-(5)Arylethenylimidazoles. J Heterocycl Chem. 1980;17:679–83.
43. Mohammad T, Kasper A, Morrison H. Urocanic acid photobiology. Purine assisted photooxidation to 1H-Imidazole-4(5)-Carboxaldehyde. Tetrahedron Lett. 1994;35(28):4903–6.
44. Papadopoulos EP, Jarrar A, Issidorides CH. Oxidations with manganese dioxide. J Org Chem. 1966;31(2):615–6.
45. Pyman FL. Derivatives of glyoxaline-4(or 5)-formaldehyde and glyoxaline-4(or 5)-carboxylic acid. A new synthesis of histidine. J Chem Soc Trans. 1916;109(197):186–202.
46. Reiter LA. Synthesis of 4(5)-Acyl-, 1-Substituted 5-Acyl-, and 1-Substituted 4-Acyl-1H-imidazoles from 4-Aminoisoxazoles. J Org Chem. 1986;52:2714–26.
47. Rosenberg H, Paul AG. Biosynthetic production of aberrant alkaloids in *Dolichothele sphaerica* (Cactaceae). J Pharm Sci. 1973;62(3):403–7.
48. Su Q, Wood JL. Regioselective N-Alkylation of 4-Formylimidazole. Synth Commun. 2000;30(18):3383–9.
49. Winter J, Retey J. A simple and efficient synthesis of N-Protected imidazole-4-carbaldehyde. Synthesis. 1994;03:245–6.
50. Takeuchi H. Raman structural markers of tryptophan and histidine side chains in proteins. Biopolymers. 2003;72:305–17.
51. Kerwin BA. Polysorbates 20 and 80 used in the formulation of protein biotherapeutics: structure and degradation pathways. J Pharm Sci. 2007;98:3200–17.
52. Yao J, Dokuru DK, Noestheden M, Park SS, Kerwin BA, Jona J, *et al.* A quantitative kinetic study of polysorbate autooxidation: the role of unsaturated fatty acid ester substituents. Pharm Res. 2009;26:2303–13.
53. Fossey J, Lefort D, Sorba J. Free Radicals in Organic Chemistry. ed.: John Wiley & Sons; 1995. p 116.
54. Guo Q, Qian SY, Mason RP. Separation and identification of DMPO adducts of oxygen-centered radicals formed from organic hydroperoxides by HPLC-ESR, ESI-MS and MS/MS. J Am Soc Mass Spectr. 2003;14:862–71.